



## ORIGINAL ARTICLE

# Cell therapy stimulates bone neoformation in calvaria defects in rats subjected to local irradiation

Ana Luisa Riul Sório<sup>1</sup> | Paula Katherine Vargas-Sanchez<sup>1</sup> | Roger Rodrigo Fernandes<sup>1</sup> |  
 Dimitrius Leonardo Pitol<sup>1</sup> | Luiz Gustavo de Sousa<sup>1</sup> | Adriano Luiz Balthazar Bianchini<sup>2</sup> |  
 Geraldo Batista de Melo<sup>3</sup> | Selma Siessere<sup>1</sup>  | Karina Fittipaldi Bombonato-Prado<sup>1</sup> 

<sup>1</sup>Department of Basic and Oral Biology, School of Dentistry of Ribeirão Preto, University of São Paulo, Ribeirão Preto, SP, Brazil

<sup>2</sup>Department of Radiotherapy, Triângulo Mineiro Federal University, Uberaba, Minas Gerais, Brazil

<sup>3</sup>Biomedical Sciences Institute, Federal University of Uberlândia, Uberlândia, Minas Gerais, Brazil

## Correspondence

Karina Fittipaldi Bombonato-Prado, Department of Basic and Oral Biology, School of Dentistry of Ribeirão Preto, University of São Paulo, Ribeirão Preto, SP, Brazil.  
 Email: karina@forp.usp.br

## Funding information

National Institute of Science and Technology, Translational Medicine, Brazil (INCT.TM); Coordenação de Aperfeiçoamento de Pessoal de Nível Superior

## Abstract

**Background:** The purpose of the study was to analyze the effect of cell therapy on the repair process in calvaria defects in rats subjected to irradiation.

**Methods:** Bone marrow mesenchymal cells were characterized for osteoblastic phenotype. Calvariae of male Wistar rats were irradiated (20 Gy) and, after 4 weeks, osteoblastic cells were placed in surgically created defects in irradiated (IRC) and control animals (CC), paired with untreated irradiated (IR) and control (C) animals. After 30 days, histological and microtomographic evaluation was performed to establish significant ( $P < 0.05$ ) differences among the groups.

**Results:** Higher alkaline phosphatase detection and activity, along with an increase in mineralized nodules, in the IRC, C and CC groups compared to the IR group, confirmed an osteoblastic phenotype. Histology showed impaired bone neoformation following irradiation, affecting bone marrow composition. Cell therapy in the IRC group improved bone neoformation compared to the IR group. Microtomography revealed increased bone volume, bone surface and trabecular number in IRC group compared to the IR group.

**Conclusion:** Cell therapy may improve bone neoformation in defects created after irradiation.

## KEYWORDS

calvaria, cell therapy, irradiation, osteoblasts, rats

## 1 | INTRODUCTION

The positive effects of head and neck radiotherapy in the treatment of neoplasias are already well known and the current challenge in this field is the evolution of this treatment, in association with a better quality of life, in order to avoid side effects. Head and neck radiotherapy may result in early side effects such as mucositis, candidiasis,

xerostomy and caries, as well as late effects such as osteoradionecrosis.<sup>1</sup> Osteoradionecrosis (ORN) is characterized by the absence of vitality in the irradiated bone, which may be exposed through the superjacent mucosa and/or skin, with no signs of repair or of primary or recurrent neoplasia and metastatic lesions over a 3 month period.<sup>2-4</sup>

Hypotheses for the occurrence of osteoradionecrosis caused by irradiation include the presence of microorganisms in the exposed

This is an open access article under the terms of the Creative Commons Attribution-NonCommercial-NoDerivs License, which permits use and distribution in any medium, provided the original work is properly cited, the use is non-commercial and no modifications or adaptations are made.

© 2019 The Authors. *Animal Models and Experimental Medicine* published by John Wiley & Sons Australia, Ltd on behalf of The Chinese Association for Laboratory Animal Sciences

surface of the bone<sup>5</sup> and endarteritis which could lead to hypoxia and hypovascularization in the affected bone tissue.<sup>4</sup> Recent advances in this field suggest that the exposed bone suffers fibroatrophy caused by a deregulation in fibroblastic activity, as well as endothelial cell injury, free radical production and inflammatory cytokine release, resulting in a hypocellular bone with little extracellular matrix formation.<sup>6-8</sup> The risk of developing head and neck ORN rests on the primary neoplasia site and its grade, the proximity of the tumor to the bone and the bone to the irradiation field, nutritional state, association with chemotherapy, acute trauma during surgical procedures, and the utilization of inadequate prosthetic devices in the oral cavity sites.<sup>9</sup> An increased risk of ORN in humans has been observed at doses higher than 60 Gy,<sup>10</sup> but other authors have demonstrated that doses equal or inferior to 50 Gy can favor its occurrence.<sup>11</sup>

ORN can be treated conservatively, using antibiotic and hyperbaric oxygen therapies, but aggressive cases are a clinical challenge that may include substantial surgical resection.<sup>12-14</sup> Mesenchymal stem cells (MSCs) have been the subject of extensive investigation in the past few decades, including in association with bone regeneration after traumas and neoplasia. They were initially shown to be present in bone marrow, but they can also be found at other sites such as spleen, umbilical cord, liver, muscles, dental pulp, blood and adipose tissue.<sup>15,16</sup> Stem cells from bone marrow are widely used mainly because they are easy to obtain and can differentiate into several cell types such as osteoblasts, chondroblasts and adipocytes.<sup>17,18</sup> It has also been suggested that MSCs possess antifibrotic, proangiogenic and immunomodulatory properties, and are thus suitable as therapeutic agents.<sup>19</sup>

Investigations into MSC therapies in individuals with osteoarthritis, cartilage defects and metabolic diseases have been described, with promising results.<sup>20</sup> Jin et al<sup>21</sup> observed in an animal model of ORN that a combined application of rat (r)MSCs and bone morphogenetic protein (BMP)-2 led to improved bone healing after post-irradiation dentoalveolar trauma in rats compared to BMP-2 applied alone. Other positive results showing increased bone deposition or preservation after the application of human adipose tissue-derived stem cells (ADSCs) to an induced mandibular osteoradionecrosis model in rats have been demonstrated using histological and radiological evaluations.<sup>14</sup> However, there are few reports of investigations demonstrating the effects of cell therapy after irradiation in bones other than femur and mandible. Thus, our hypothesis was that osteoblastic cell therapy in calvaria defects after local irradiation may favor bone neoformation and reduce its side effects.

## 2 | MATERIALS AND METHODS

The experimental protocol was approved by Ethics Committee for Animal Experimentation of the University of São Paulo, Ribeirão Preto, São Paulo, Brazil (permit number 2015.1.765.58.5). All applicable institutional and/or national guidelines for the care and use of animals were followed. Thirty-six Wistar male rats weighing approximately 300 g were subjected to irradiation previously to calvaria

surgical defects (n = 18) or served as controls (n = 18). The rats were previously subjected to surgery to achieve similar calvaria defects. Another 4 Wistar male rats were used for collection of femoral bone marrow cells to characterize osteoblastic phenotype after chemical differentiation and to obtain cells to treat the defects. The animals were selected from the Central Vivarium of the University (USP-Ribeirão Preto) and were kept in polyethylene boxes with three animals per box. The temperature was maintained between 23 and 24°C and the boxes were lit for 12 hours per day. Throughout the experiment, the animals received a standard solid diet and water ad libitum.

### 2.1 | Cell culture for osteoblastic phenotype characterization

Mesenchymal bone marrow cells obtained from femur medullary canals of four male rats were cultured in basal growth medium  $\alpha$ -MEM (Gibco) supplemented with 10% fetal bovine serum (Gibco), 0.3  $\mu$ g/mL fungizone (Gibco) and 50  $\mu$ g/mL gentamycin (Gibco). After reaching subconfluence, the cells were seeded into 24-well cell culture plates at a concentration of  $2 \times 10^4$  cells per well, and divided in two experimental groups. Group 1 was cultured in basal growth medium (MEM) and group 2 was cultured in osteogenic medium (MTS), ie MEM with the addition of  $10^{-7}$  M dexamethasone (Sigma), 5  $\mu$ g/mL ascorbic acid, and 2.16 g/mL  $\beta$ -glycerophosphate. Cells were maintained in a humidified atmosphere at 37°C with 5% CO<sub>2</sub>, and medium change occurred every 3 days. The osteoblastic phenotype characterization was performed as described in the following sections.

### 2.2 | Alkaline phosphatase (ALP) activity

After 10 days of cell culture, the medium was removed from the plates and the wells were washed three times with PBS (Gibco) heated to 37°C. The wells were then filled with 1 mL of 0.1% sodium lauryl sulfate solution (Sigma) for 30 minutes. ALP activity was determined as the release of thymolphthalein by hydrolysis of the substrate thymolphthalein monophosphate, using the commercial kit (Labtest Diagnostica SA, Lagoa Santa, MG, Brazil) and following the manufacturer's instructions. The absorbance was measured in a spectrophotometer (Bio-Tek) (590 nm). The activity was normalized to total protein content.

### 2.3 | *In situ* ALP detection

*In situ* ALP detection was also performed after 10 days. Cells were washed twice with PBS at 37°C. Then, 320 mg of Trizma® Pre-set crystals (Sigma-Aldrich) were dissolved in 20 mL of deionized water. From this solution, 18 mL were added to 2 mL of dimethylformamide (Merck) with 8 mg Naphthol (Sigma-Aldrich). This was followed by addition of 7 mg of Fast Red reagent (Sigma-Aldrich) to the final work solution. Finally, cells were incubated in 1 mL of this solution in a humidified atmosphere at 37°C with 5% CO<sub>2</sub> for 30 minutes and then removed from the wells for subsequent analysis.

## 2.4 | Mineralized matrix formation

The detection of mineralized nodules was performed after 21 days by means of Alizarin Red S (Sigma-Aldrich) staining for areas rich in calcium. Attached cells were fixed in 10% formalin at 4°C, for 2 hours. After fixation, specimens were dehydrated through a graded series of alcohol solutions, followed by staining with 2% Alizarin Red S, pH 4.2, for 10 minutes. The calcium content was evaluated using a previously described colorimetric method.<sup>22</sup>

## 2.5 | *In vivo* irradiation

The irradiation protocol was performed in the Radiotherapy Department of Medicine, School of Triângulo Mineiro (Uberaba, MG, Brazil), using a Varian 600 C Linear Accelerator equipment (Varian Medical Systems, CA, EUA). Before irradiation, the rats were weighed and anesthetized by an intramuscular injection of xylazine (10 mg/kg) and ketamine (75 mg/kg) (Agibrands do Brasil LTDA, Campinas, SP, Brazil). The Linear Accelerator used was set to deliver a dose range of 2.5 Gy/minute; thus, 8 minutes of exposure were necessary to achieve 20 Gy in the left hemisphere of calvaria of the selected animals.<sup>23</sup> Regarding the frequency of irradiation, the Linear Accelerator has an acceleration potential of 6 MV (megavolts), with maximal energy of the beam produced being 6 MeV, equivalent to  $9.6 \times 10^{-13}$  joules. We used the equation known as the Planck-Einstein relation, which gives the electromagnetic radiation energy as its frequency multiplied by the Planck constant:

$$E = h \times f$$

where E = electromagnetic radiation energy in joules;  $h = 6.62 \times 10^{-34}$  Js (Planck constant); f = frequency of electromagnetic radiation in hertz.

We can state that the maximum frequency of X-ray beams produced by the equipment was  $1.45 \times 10^{21}$  Hz.

## 2.6 | Surgical procedure for producing calvaria defects

Four weeks after irradiation, bone defects were created in both irradiated and control animals. They were weighed and anesthetized with an intraperitoneal injection of ketamine (75 mg/kg) (União Química Farmacêutica Nacional S/A, Embu-Guaçu, SP, Brazil) and xylazine (10 mg/kg) (Hertape Calier, Juatuba, MG, Brazil). The animals were then subjected to trichotomy, antisepsis and a sagittal incision (1 cm long) to expose the intended bone area. A circular bone defect 5 mm in diameter was made in the central region of the left parietal bone using a trephine drill (Neodent, Curitiba, PR, Brazil) and an electric implant motor (Dentscler, Ribeirão Preto, SP, Brazil) running at 900 g. The bone defect was performed under constant irrigation with sterile saline solution (0.9%). The animals were then divided in 4 groups: control (C), control + cell therapy

(CC), irradiated (IR) and irradiated + cell therapy (IRC). The osteoblastic cells were removed from the culture bottles with EDTA and collagenase, centrifuged and suspended in new medium. After cell counting,  $5 \times 10^5$  cells suspended in gel vehicle were placed inside the surgical defects of rats in the cell therapy groups. The incisions were then sutured with 4.0 silk thread (Ethicon, Johnson & Johnson, São José dos Campos, SP, Brazil). All animals received a single dose intramuscular injection of Banamine painkiller (1.1 mg/kg; MSD Saúde Animal, São Paulo, SP, Brazil) and Pentabiotico Veterinário, Pequeno Porte (0.1 mL/100 g; Fort Dodge®, Campinas, SP, Brazil). The animals were sacrificed after 4 weeks and the calvaria were collected and processed for histology and microCT analysis.

## 2.7 | MicroCT morphometric analysis

Calvaria samples (n = 5) were fixed in 4% buffered formalin solution (pH 7) for 2 days and transferred to a 70% ethanol solution for 3 days. The microtomographic analysis was performed using a Skyscan 1,172 microCT scanner (Skyscan, Kontich, Belgium) operating with 100 kV X-rays detected by a 11-megapixel camera with a resolution of up to 1  $\mu$ m. Data were acquired through the reconstruction of the two-dimensional (2D) projection images into a 3D volumetric image stack, performed using the software NRecon (Bruker microCT, Kontich, Belgium). After the reconstruction, the bone defect area was analyzed according to the following parameters: bone volume (mm<sup>3</sup>), bone surface (mm<sup>2</sup>), trabecular number (1/mm), trabecular thickness (mm), trabecular separation (mm), connectivity density (1/mm<sup>3</sup>), total porosity (%) and open porosity (%).<sup>24</sup>

## 2.8 | Histological processing

Calvaria samples containing the defect site (n = 4) were collected and fixed in buffered (pH 7) 10% formaldehyde solution for 24 hours. The specimens were then washed in running water and decalcified with a solution containing 10% EDTA for 30 days. This solution was replaced every 2 days and neutralized with 5% sodium sulfate. The specimens were then dehydrated in a series of increasingly concentrated ethanol solutions: 70% overnight, then 80%, 85%, 90%, 95% and finally 100% for 2 hours each. The specimens were then washed with xylol and embedded in paraffin. Longitudinal semiserial sections 6  $\mu$ m thick were stained with hematoxylin and eosin. The analysis was carried out using a Leica DM4000B light microscope (Leica, Bensheim, Germany) fitted with a Leica DFC310FX camera.

## 2.9 | Statistical analysis

After applying a Shapiro-Wilk normality test, the results were analyzed using analysis of variance (ANOVA) or a Mann-Whitney test, with the level of significance set at 5% ( $P \leq 0.05$ ), using the software GraphPad Prism.

### 3 | RESULTS

#### 3.1 | Cell culture for osteoblastic phenotype characterization

Bone marrow cells cultured in osteogenic medium (MTS) showed an increase in alkaline phosphatase activity (Figure 1A) and its in situ detection (Figure 1B) after 10 days. Qualitative evaluation of mineralized matrix formation after 21 days also demonstrated a higher deposition of calcified nodules in the group in contact with osteogenic medium (Figure 1C).

#### 3.2 | Histological analysis

Fragments of calvaria surrounding the defects were submitted to qualitative analysis after histological processing. The control group (C) showed bone from the remaining borders, delimited by active osteoblasts adjacent to mineralized matrix. The defect was partially filled by bone tissue adjacent to connective tissue rich in blood vessels (Figure 2A). The control group that received osteoblastic cells

(CC) was histologically similar to group C, but with an increase in bone neoformation at the defect borders (Figure 2B). The irradiated animals (group IR) showed minimal bone tissue neoformation in the region of the defect, with an osteoclast layer adjacent to resorption areas and few active osteoblasts on the matrix surface (Figure 2C). In contrast, therapy with osteoblastic cells after irradiation (group IRC) promoted an increase in bone neoformation, with an active osteoblast layer on the surface of the bone matrix (Figure 2D). Calvaria bone marrow in groups C and CC showed cellularity, and the presence of hematopoietic progenitor cells and megacariocytes (Figure 3A,B). This scenario was not observed in the medulla of the IR group, which showed a predominance of adipocytes and few progenitor hematopoietic cells (Figure 3C). Cell therapy with osteoblastic cells in the IRC group presented bone marrow similar to control groups (Figure 3D).

#### 3.3 | Microtomographic (MicroCT) evaluation

The analysis of 3D image reconstruction demonstrated that bone neoformation started from the borders of the defect, with similar morphologies in the control groups (Figure 4A,B), minimal bone formation in the calvaria defects of irradiated rats (Figure 4C) and significant de novo bone formation after therapy with osteoblastic cells in the IRC group (Figure 4D). Quantitative analysis was performed using eight parameters, four of which showed statistically significant differences among the experimental groups (Figure 5). Bone volume was decreased in the IR group, with a significant increase after the insertion of osteoblastic cells ( $P = 0.0058$ ), similar to that in group C. Bone surface was significantly decreased in the IR group compared to the control group (C), and the presence of osteoblastic cells significantly increased this parameter, to a similar extent to that in groups C and CC ( $P = 0.0144$ ). Trabecular thickness showed a significant decrease in the IR group compared to groups C and CC ( $P = 0.023$ ), and a non-significant increase in the IRC group. Trabecular number also decreased in the IR group compared to all other groups ( $P = 0.0020$ ), which were similar to each other. Trabecular separation was similar among all experimental groups ( $P = 0.5762$ ), as was total porosity ( $P = 0.1469$ ). Despite the absence of statistical significance for connectivity density differences ( $P = 0.0759$ ), this parameter was increased in IRC group compared to IR and was similar to group C. Open porosity was similar among all experimental groups ( $P = 0.0793$ ).

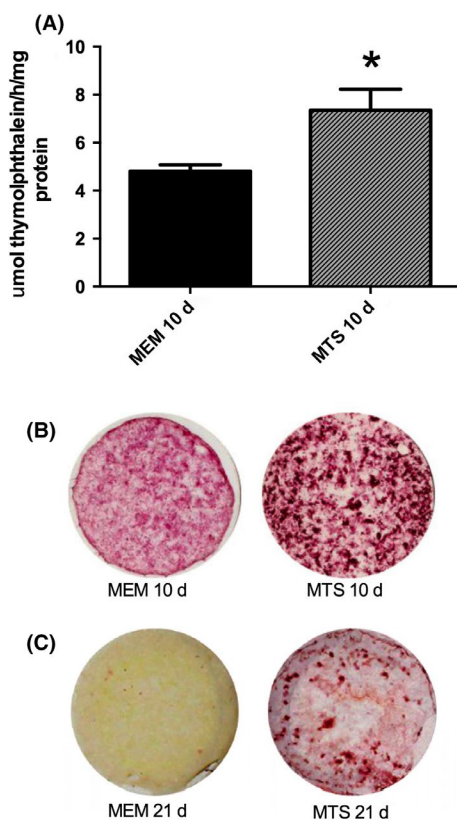


**FIGURE 1** A, Alkaline phosphatase (ALP) activity of bone marrow mesenchymal cells cultured in basal growth medium (MEM) and osteogenic medium (MTS) after 10 d of culture. B, In situ ALP detection in bone marrow mesenchymal cells cultured in basal growth medium (MEM) and osteogenic medium (MTS) after 10 d of culture. C, Detection of mineralization nodules in bone marrow mesenchymal cells cultured in basal growth medium (MEM) and osteogenic medium (MTS) after 21 d of culture. \*Significant difference at  $P < 0.05$ ; Mann-Whitney test

### 4 | DISCUSSION

The present study demonstrates the benefits of cell therapy in the repair process in calvaria defects in rats submitted to irradiation. The irradiated animals received a single dose of 20 Gy, which is equivalent to a biological dose of 60 Gy in a conventional irradiation fraction protocol in a human being. According to the literature, the risk of bone tissue necrosis occurring in humans starts at 50 Gy.<sup>25,26</sup> Histological analysis of the irradiated calvaria in the present study revealed osteoblast and osteocyte reduction, a decrease in vascularization, and

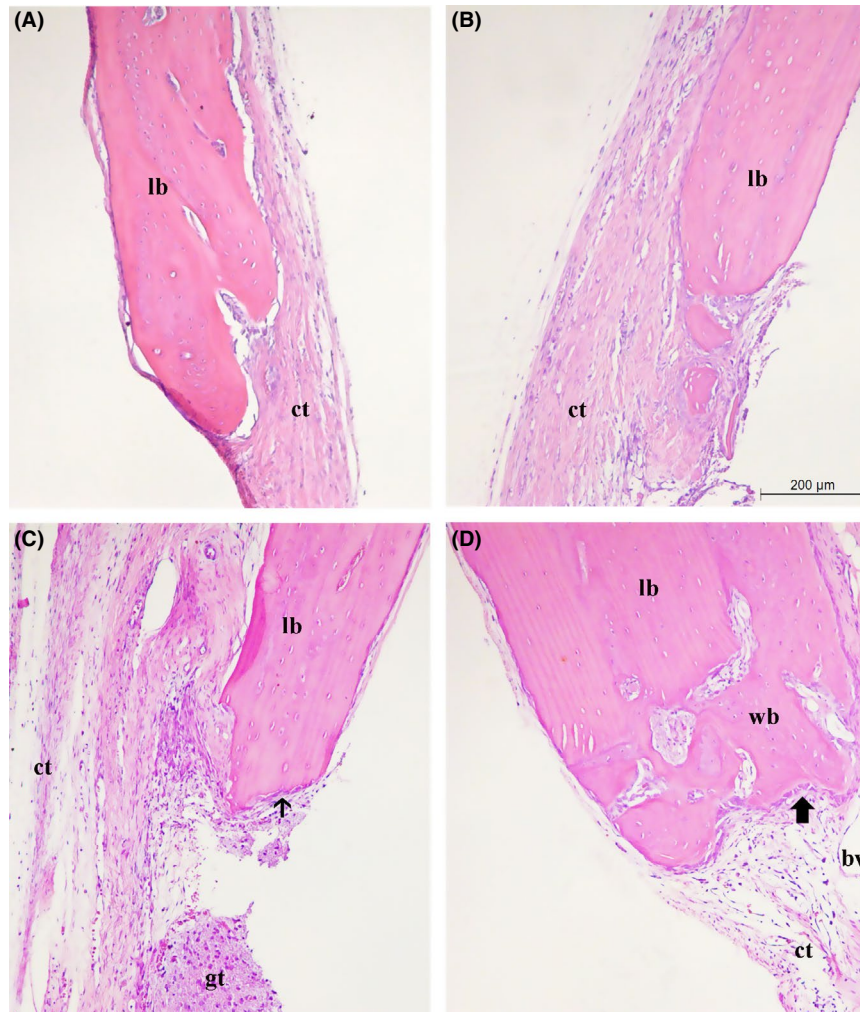


**FIGURE 2** Histological sections of calvaria defect sites. A, Control group shows defect borders with lamellar bone (lb) and connective tissue (ct). B, Control group + cell therapy (CC) shows lamellar bone (BT) with organized connective tissue (ct). C, Irradiated group (IR) shows lamellar bone with osteoclast layer adjacent to Howship lacunae (thin arrow), disorganized connective tissue (ct) and granulation tissue (gt). D, Irradiated group + cell therapy (IRC) shows lamellar bone (lb) and woven bone (wb) with an osteoblast layer (thick arrow), blood vessels (bv) and connective tissue (CT). Hematoxylin and eosin stain. Scale bar = 200  $\mu\text{m}$

bone marrow retraction, with an increase in the number of adipocytes. These findings have also been reported by other researchers,<sup>4</sup> who demonstrated the presence of hyperemia, endarteritis, thrombosis, hypocellularity, adipocytes in bone marrow, and fibrosis. A single dose of 20 Gy in rat mandibles increased osteoclast and decreased osteoblast numbers compared to control animals, with a bone volume of 13.8% in the irradiated group compared to 65.9% of control group.<sup>27</sup>

Osteoradionecrosis in bones such as mandible is commonly associated to periodontal diseases, dental extraction, surgeries and traumas.<sup>9</sup> Thus, studies aimed at creating an experimental model of ORN for evaluating new therapies can also establish protocols for *in vivo* traumas. In the present investigation, a surgical trauma protocol was chosen in order to create an optimal and repeatable defect size in the calvaria, to develop an experimental model of ORN.<sup>28</sup> Circular bone defects of 5 mm in the calvaria in adult rats were performed in this study as reports show that such defects provide an adequate model for evaluating bone neoformation in the craniofacial region.<sup>29</sup>

The experimental period of 30 days in this study was chosen in line with other reports.<sup>30</sup> During this period a layer of osteoblasts on neoformed bone from irradiated animals was observed, while in the irradiated animals only non-calcified connective tissue was present. Moreover, therapy with osteoblastic cells placed inside the defect after irradiation stimulated bone neoformation.

Other research has demonstrated the positive effect of cell therapy on bone defects, using different types of cells at different bone defect sites.<sup>21,31</sup> Mesenchymal cells may help in the formation of new bone tissue by stimulating the remaining cells to produce growth factors,<sup>32</sup> a variety of which, eg bone morphogenetic proteins (BMPs), insulin-like growth factor 1 and 2 (IGF1/2), transforming growth factor beta 1 (TGF $\beta$ 1), platelet derived growth factor (PDGF) and fibroblast growth factor (FGF), are produced by osteogenic cells and are functionally involved in bone repair.<sup>33-35</sup> Our histological analysis showed that irradiation promoted injuries to bone tissue adjacent to the defect border, with resorption areas and disorganized

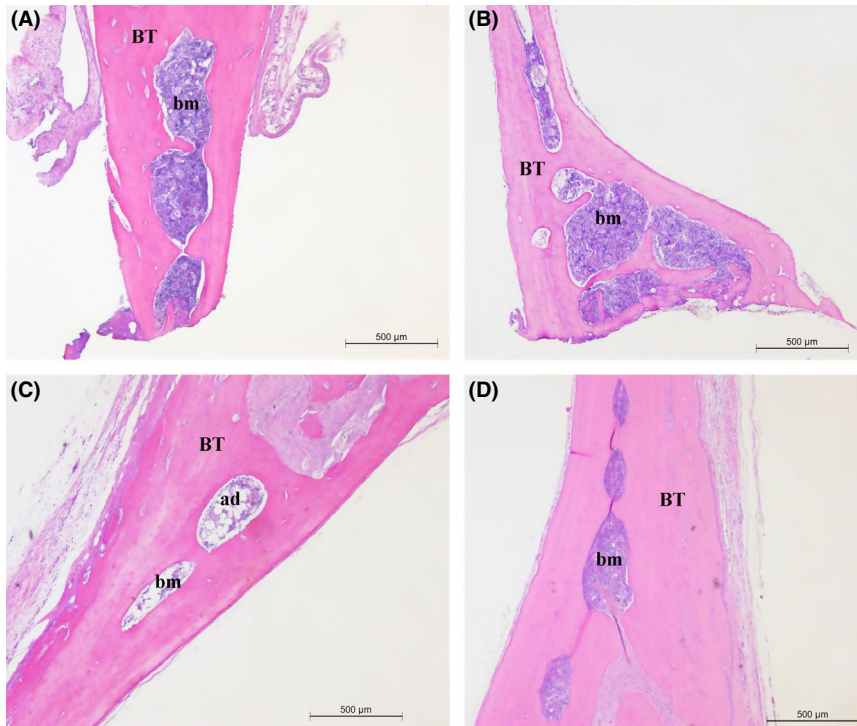


**FIGURE 3** Histological sections of calvaria defect sites. A, Control group (C). B, Control group + cell therapy (CC) showing bone tissue (BT) and bone marrow (bm). C, Irradiated group (IR) showing adipocytic bone marrow (ad). D, Irradiated + cell therapy (IRC). Hematoxylin and eosin stain. Scale bar = 500  $\mu\text{m}$

connective tissue, and reduced and adipocytic bone marrow, consistent with other investigations.<sup>21,28</sup> *In vivo* studies have shown that radiation may decrease the number of osteocytes, resulting in empty lacunae, and leading to replacement of bone by non-calcified connective tissue.<sup>36</sup> In our study, therapy with osteoblastic cells promoted bone neoformation at the defect borders, indicating the establishment of new osteoblasts on the surface of remaining

bone. Previous reports have suggested that the positive effects of cell therapy may be due to an upregulation of genes associated with bone metabolism, such as BMP-2, and downregulation of PPAR- $\gamma$ , which is associated with adipocytic differentiation.<sup>37</sup> Others have demonstrated that systemic infusion with mesenchymal stem cells (MSCs) prevents and heals bisphosphonate-related osteonecrosis of the jaw, possibly via induction of peripheral tolerance, shown as

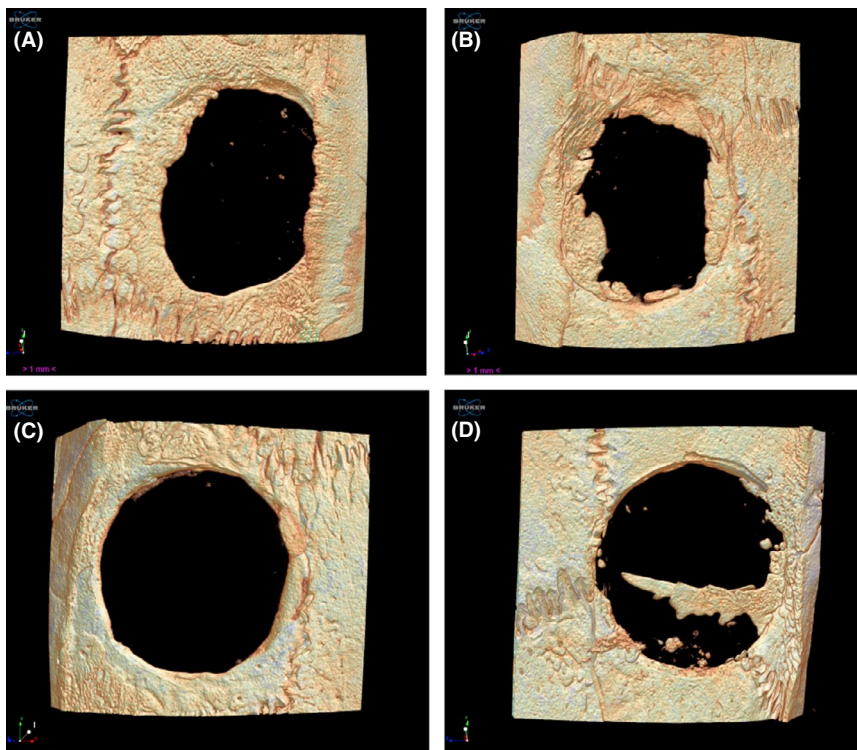


**FIGURE 4** Microtomographic 3D reconstruction images from calvaria defects of experimental groups. A, Control (C). B, Control + cell therapy (CC); C, Irradiated (IR). D, Irradiated + cell therapy (IRC)

an inhibition of inflammatory T-helper-producing interleukin 17 cells (Th17) and an increase in adaptive regulatory T cells (Treg).<sup>38</sup>

Quantitative analysis was performed using computerized microtomography to complement the information obtained by histological analysis. A great advantage of this method is the high number of sections obtained, enabling visualization of differences in the samples and collection of data based on pre-established parameters. It also allows preservation of the samples and reconstruction of 3D images.<sup>39</sup> Nevertheless, analysis of histological sections is also important to provide a precise study of cell morphology, tissue organization

and inflammatory infiltrate. Of the eight selected microCT analysis parameters, four—bone volume, bone surface, trabecular number and trabecular thickness—were significantly different in calvaria defects receiving cell therapy after irradiation. The data obtained suggest that the presence of osteoblastic cells stimulated bone neoformation after irradiation, with volume and trabecular architecture changes similar to the control groups used in this study. Other investigations using different cell types also reported an increase of bone neoformation based on microCT analysis. Jin et al<sup>21</sup> observed that treatment with cells associated with BMP-2 after 4 weeks of

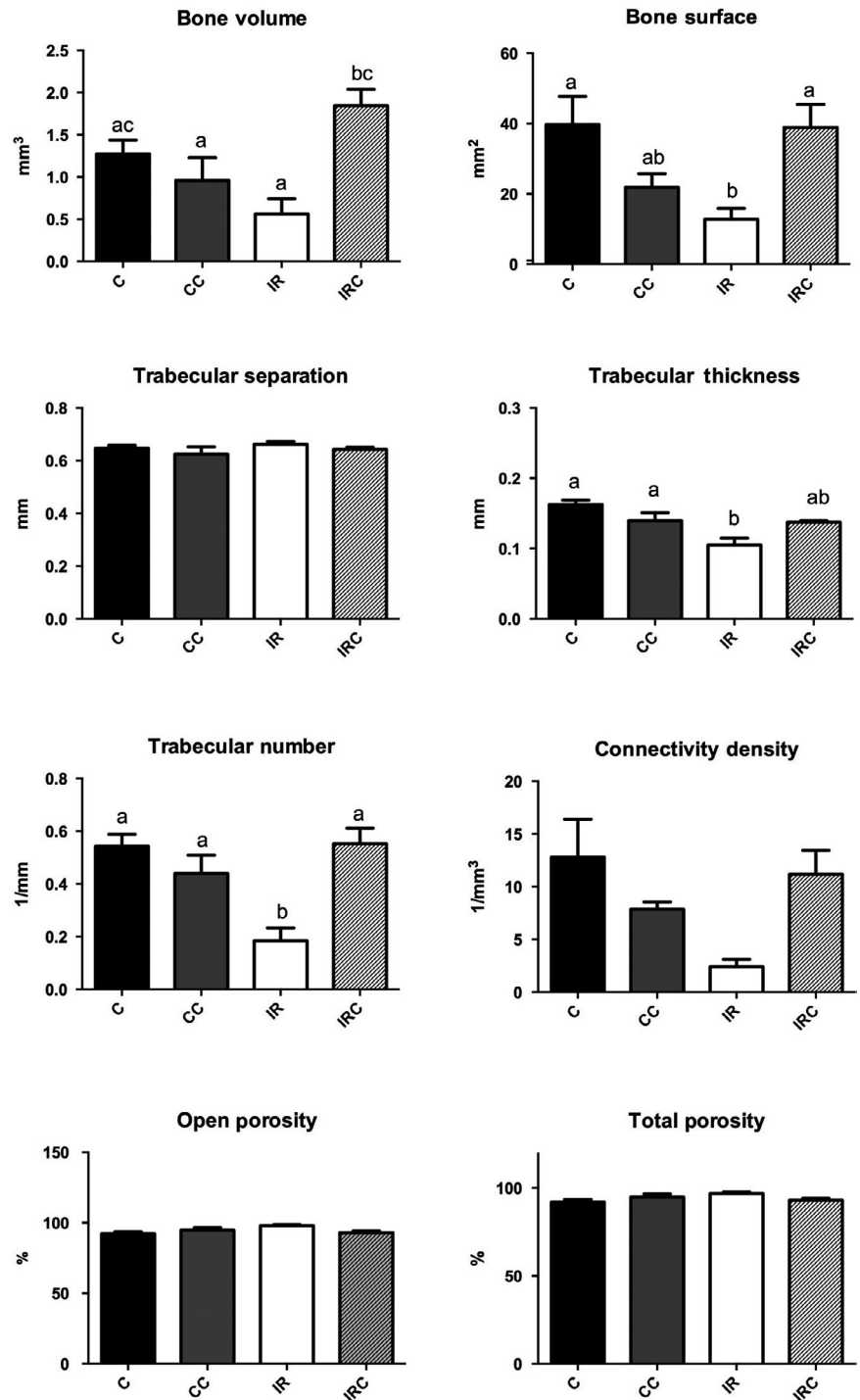


**FIGURE 5** Bone volume, bone surface, trabecular separation/thickness/number, connectivity density, open porosity and total porosity microtomographic quantitative parameters evaluated in control (C), control + cell therapy (CC), irradiated (IR) and irradiated + cell therapy (IRC) groups. Letters above error bars indicate statistically significant differences ( $P < 0.05$ ; one-way ANOVA)

ORN induction increased bone volume, bone mineral density, trabecular number and trabecular separation. Janus et al<sup>14</sup> described an increase of 36% in bone volume in rats receiving cells derived from adipose tissue after 8 weeks of ORN induction in the mandible compared to rats receiving saline solution. Vascularization, analyzed using histological and microtomography parameters (open porosity), was not affected by cell therapy, possibly because of the time point selected. Earlier time points might have produced a more differentiated comparison of angiogenesis among the studied groups.

The results of this investigation suggest a positive effect of using osteoblastic cells from bone marrow as a therapy to promote bone neoformation in calvaria defects after irradiation. These findings may contribute to therapeutic resolution of ORN, offering a better quality of life to patients that present this side effect as a consequence of radiotherapy.

## ACKNOWLEDGEMENTS

The authors would like to thank Coordination for the Improvement of Higher Education Personnel (CAPES) for funding and National Institute of Science and Technology, Translational Medicine, Brazil.

## CONFLICT OF INTEREST

None.

## AUTHOR CONTRIBUTIONS


KFBP and SS conceived and designed the study. LGS, ALRS and PKVS performed the animal surgeries. RRF, ALRS and PKVS performed the in vitro studies. ALBB performed the local irradiation. GBM conceived the vehicle used to carry the cells. DLP and ALRS performed the histological processing. ALRS acquired the histological images and wrote the main manuscript. KFBP and ALRS performed and analyzed the data.

## ETHICAL APPROVAL

All applicable international, national, and/or institutional guidelines for the care and use of animals were followed.

## ORCID

Selma Siessere  <https://orcid.org/0000-0001-9756-3771>

Karina Fittipaldi Bombonato-Prado  <https://orcid.org/0000-0002-0267-7643>

## REFERENCES

- Chrcanovic BR, Reher P, Sousa AA, Harris M. Osteoradionecrosis of the jaw—a current overview—part 1: physiopathology and risk and predisposing factors. *Oral Maxillofac Surg.* 2010;14:3-16.
- Marx RE. Osteoradionecrosis: a new concept of its pathophysiology. *J Oral Maxillofac Surg.* 1983;41:283-288.
- Rahman S, Maillou P, Barker D, Donachie M. Radiotherapy and the oral environment the effects of radiotherapy on the hard and soft tissues of the mouth and its management. *Eur J Prosthodont Restor Dent.* 2013;21:80-87.
- Curi MM, Cardoso CL, de Lima HG, Kowalski LP, Martins MD. Histopathologic and histomorphometric analysis of irradiation injury in bone and the surrounding soft tissues of the jaws. *J Oral Maxillofac Surg.* 2016;74:190-199.
- Meyer I. Infectious diseases of the jaws. *J Oral Surg.* 1970;28:17-26.
- Delanian S, Lefaix JL. The radiation-induced fibroatrophic process: therapeutic perspective via the antioxidant pathway. *Radiother Oncol.* 2004;73:119-131.
- O'Dell K, Sinha U. Osteoradionecrosis. *Oral Maxillofac Surg Clin North Am.* 2011;23:455-464.
- Deshpande SS, Gallagher KK, Donneys A, et al. Stem cells rejuvenate radiation-impaired vasculogenesis in murine distraction osteogenesis. *Plast Reconstr Surg.* 2015;135:799-806.
- Jacobson AS, Buchbinder D, Hu K, Urken ML. Paradigm shifts in the management of osteoradionecrosis of the mandible. *Oral Oncol.* 2010;46:795-801.
- Lee IJ, Koom WS, Lee CG, et al. Risk factors and dose-effect relationship for mandibular osteoradionecrosis in oral and oropharyngeal cancer patients. *Int J Radiat Oncol Biol Phys.* 2009;75:1084-1091.
- Curi MM, Dib LL. Osteoradionecrosis of the jaws: retrospective study of the background factors and treatment in 104 cases. *J Oral Maxillofac Surg.* 1997;35:540-544.
- Aldunate J, Coltro PS, Busnardo FF, Ferreira MC. Osteoradionecrosis in face: pathophysiology, diagnosis and treatment. *Rev Bras Cir Plást.* 2010;25:381-387.
- Xu J, Zheng Z, Fang D, et al. Early-stage pathogenic sequence of jaw osteoradionecrosis in vivo. *J Dent Res.* 2012;91:702-708.
- Janus JR, Jackson RS, Lees KA, et al. Human adipose-derived mesenchymal stem cells for osseous rehabilitation of induced osteoradionecrosis: a rodent model. *Otolaryngol Head Neck Surg.* 2017;156:616-621.
- Beloti MM, Sicchieri LG, de Oliveira PT, Rosa AL. The influence of osteoblast differentiation stage on bone formation in autogenously implanted cell-based poly (lactide-co-glycolide) and calcium phosphate constructs. *Tissue Eng Part A.* 2012;18:999-1005.
- Wang Y, Yao J, Yuan M, Zhang Z, Hu W. Osteoblasts can induce dental pulp stem cells to undergo osteogenic differentiation. *Cytotechnology.* 2013;65:223-231.
- In't Anker PS, Noort WA, Scherjon SA, et al. Mesenchymal stem cells in human second-trimester bone marrow, liver, lung, and spleen exhibit a similar immunophenotype but a heterogeneous multilineage differentiation potential. *Haematologica.* 2003;88:845-852.
- Santos T, Abuna R, Lopes HB, et al. Association of mesenchymal stem cells and osteoblasts for bone repair. *Regen Med.* 2015;10:127-133.
- Sensebé L, Bourin P, Tarte K. Good manufacturing practices production of mesenchymal stem/stromal cells. *Hum Gene Ther.* 2011;22:19-26.
- Chen K, Teh TK, Ravi S, Toh SL, Goh JC. Osteochondral interface generation by rabbit marrow stromal cells and osteoblasts coculture. *Tissue Eng Part A.* 2012;18:1902-1911.
- Jin IG, Kim JH, Wu HG, Kim SK, Park Y, Hwang SJ. Effect of bone marrow-derived stem cells and bone morphogenetic protein-2 on treatment of osteoradionecrosis in a rat model. *J Craniomaxillofac Surg.* 2015;43:1478-1486.
- Gregory CA, Gunn WG, Peister A, Prockop DJ. An alizarin red-based assay of mineralization by adherent cells in culture: comparison with cetylpyridinium chloride extraction. *Anal Biochem.* 2004;329:77-84.



23. Lerouxel E, Moreau A, Bouler JM, et al. Effects of high doses of ionising radiation on bone in rats: a new model for evaluation of bone engineering. *Br J Oral Maxillofac Surg*. 2009;47:602-607.
24. Parfitt AM, Drezner MK, Glorieux FH, et al. Bone histomorphometry: standardization of nomenclature, symbols, and units. Report of the ASBMR Histomorphometry Nomenclature Committee. *J Bone Miner Res*. 1987;2:595-610.
25. Vissink A, Burlage FR, Spijkervet FK, Jansma J, Coppes RP. Prevention and treatment of the consequences of head and neck radiotherapy. *Crit Rev Oral Biol Med*. 2003;14:213-225.
26. De Felice F, Musio D, Tombolini V. Osteoradionecrosis and intensity modulated radiation therapy: an overview. *Crit Rev Oncol Hematol*. 2016;107:39-43.
27. Tamplen M, Trapp K, Nishimura I, et al. Standardized analysis of mandibular osteoradionecrosis in a rat model. *Otolaryngol Head Neck Surg*. 2011;145:404-410.
28. Bléry P, Espitalier F, Hays A, et al. Development of mandibular osteoradionecrosis in rats: Importance of dental extraction. *J Craniomaxillofac Surg*. 2015;43:1829-1836.
29. Bosch C, Melsen B, Vargervik K. Importance of the critical-size bone defect in testing bone-regenerating materials. *J Craniofac Surg*. 1998;9:310-316.
30. Scalize PH, Bombonato-Prado KF, de Sousa LG, et al. Poly(Vinylidene Fluoride-Trifluorethylene)/barium titanate membrane promotes de novo bone formation and may modulate gene expression in osteoporotic rat model. *J Mater Sci Mater Med*. 2016;27:180.
31. Manimaran K, Sankaranarayanan S, Ravi VR, Elangovan S, Chandramohan M, Perumal SM. Treatment of osteoradionecrosis of mandible with bone marrow concentrate and with dental pulp stem cells. *Ann Maxillofac Surg*. 2014;4:189-192.
32. Handschel J, Meyer U. Infection, vascularization, remodelling—are stem cells the answers for bone diseases of the jaws? *Head Face Med*. 2011;7:5.
33. Tsumaki N, Tanaka K, Arikawa-Hirasawa E, et al. Role of CDMP-1 in skeletal morphogenesis: promotion of mesenchymal cell recruitment and chondrocyte differentiation. *J Cell Biol*. 1999;144:161-173.
34. Gruber R, Mayer C, Schulz W, et al. Stimulatory effects of cartilage-derived morphogenetic proteins 1 and 2 on osteogenic differentiation of bone marrow stromal cells. *Cytokine*. 2000;12:1630-1638.
35. Reddi AH. Cartilage morphogenetic proteins: role in joint development, homeostasis, and regeneration. *Ann Rheum Dis*. 2003;62:Suppl2:ii73-78.
36. Lambert EM, Gunn GB, Gidley PW. Effects of radiation on the temporal bone in patients with head and neck cancer. *Head Neck*. 2016;38:1428-1435.
37. Fu Q, Tang N-N, Zhang Q, et al. Preclinical study of cell therapy for osteonecrosis of the femoral head with allogenic peripheral blood-derived mesenchymal stem cells. *Yonsei Med J*. 2016;57:1006-1015.
38. Kikuri T, Kim I, Yamaza T, et al. Cell-based immunotherapy with mesenchymal stem cells cures bisphosphonate-related osteonecrosis of the jaw-like disease in mice. *J Bone Miner Res*. 2010;25:1668-1679.
39. Rühli FJ, Kuhn G, Evison R, Müller R, Schultz M. Diagnostic value of microCT in comparison with histology in the qualitative assessment of historical human skull bone pathologies. *Am J Phys Anthropol*. 2007;133:1099-1111.

**How to cite this article:** Sório ALR, Vargas-Sanchez PK, Fernandes RR, et al. Cell therapy stimulates bone neoformation in calvaria defects in rats subjected to local irradiation. *Animal Model Exp Med*. 2019;2:169-177. <https://doi.org/10.1002/ame2.12073>